A Sensitivity Study Approach to Improve the Sound Transmission Loss Performance of Vibro-acoustic Metamaterials with Embedded Helmholtz Resonators

Kenneth Leung[1], Felix Langfeldt[1]

[1] *Institute of Sound and Vibration Research, University of Southampton, Email: kenneth.leung@soton.ac.uk*

Introduction

Acoustic metamaterials (AMM), which usually consist of resonators that are periodically attached onto a partition layer (or the *host structure*) offer a high sound transmission loss (TL) near the resonance frequencies of the resonators, which can greatly exceed the corresponding mass-law TL. One common AMM design is a vibroacoustic metamaterial consisting of a cantilever beam with an attached end mass [1]. However, the TL improvement of these vibroacoustic metamaterials is not only limited to a narrow frequency band, but the resonators also introduce a partition resonance which leads to poorer TL performance at higher frequencies [1]. Various strategies have been documented in literature to tackle the two problems mentioned above [2, 3, 4], but these solutions require adding mass to the partition. Other works in the literature suggest that by embedding Helmholtz resonators in partition layers the TL performance of partitions can be enhanced, albeit offering only a narrowband TL improvement in the case of single-layer partitions [5].

The AMM design studied in this paper consists of a cantilever-type resonator with embedded Helmholtz resonators, as shown in Figure 1. This metamaterial design extends the bandwidth of performance by tuning the embedded Helmholtz resonator to a different resonance frequency than the cantilever, without introducing additional mass or vibro-acoustic resonators. The main question to answer in this paper is: How can we design this metamaterial to best achieve a broadband TL improvement above the corresponding mass-law? This paper will be structured as follows. Firstly, an analytical approach to model the metamaterial is introduced, based on homogenising the metamaterial as a multi-layered effective medium. Next, a sensitivity study is performed to understand the effect of key parameters on the transmission loss performance of the metamaterial. Conclusions are drawn in the end to summarise the work and the key findings of this paper.

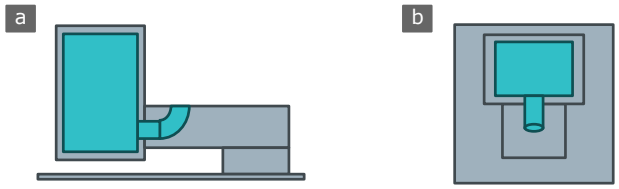

Figure 1: A schematic of a unit cell of the cantilever resonator-type acoustic metamaterial with an embedded Helmholtz resonator. (a) Side view; (b) Top view.

Effective Medium Model

The effective medium theory, a common analytical modelling tool for metamaterials, is applied in this work by treating the metamaterial as a homogenised medium with equivalent material properties. This method is built on the assumption that the size of the resonator is much smaller than the acoustic wavelength within the frequency range of interest. The metamaterial in this work can be represented by two effective media arranged in parallel: the structural vibration of the metamaterial plate is represented by an effective plate with frequency-dependent mass density $\rho_{\mathrm{eff,cl}}$ and the Helmholtz resonance mechanism is represented by an effective fluid with frequency-dependent bulk modulus $K_{\mathrm{eff,hr}}$, where the bulk modulus is a measure for the fluid stiffness.

To model the effective mass density of the effective plate, the metamaterial can be treated as a two degree-of-freedom (DoF) system, where the lumped masses are the host structure and the cantilever moving mass, and the connecting lumped spring element is the cantilever beam. By rearranging the equations of motion, this mechanical system can be represented by an effective mass density of

$$\rho_{\mathrm{eff,cl}} = \frac{m_0''}{d_{\mathrm{cl}}}\left[1 + \phi_{\mathrm{cl}}\frac{\Omega_{\mathrm{cl}}^2}{1 + 2\mathrm{j}\zeta_{\mathrm{cl}}\Omega_{\mathrm{cl}} - \Omega_{\mathrm{cl}}^2}\right] \quad [3], \qquad (1)$$

where m_0'' is the static surface mass density of the metamaterial unit cell, $\phi_{\mathrm{cl}} = m_{\mathrm{cl}}/(Sm_0'')$ is the cantilever mass ratio, defined as the quotient between the moving mass of the resonator m_{cl} and the static surface mass. S is the surface area the unit cell. ζ_{cl} is the damping ratio of the resonator. $\Omega_{\mathrm{cl}} = f/f_{\mathrm{cl}}$ is the normalised frequency, where f is frequency and f_{cl} is the structural resonance frequency. The density and thickness of the host structure are ρ_{cl} and d_{cl}, respectively. At frequencies near the structural resonance, the effective plate has an effective mass that is much greater than the static mass, which results in superior transmission loss.

The behaviour of the fluid surrounding the resonator due to the Helmholtz resonator is modelled as an equivalent fluid with effective bulk modulus $K_{\mathrm{eff,hr}}$, calculated by

$$K_{\mathrm{eff,hr}} = \frac{K_0}{1 - \phi_{\mathrm{hr}} + \frac{\phi_{\mathrm{hr}}}{1 + 2\mathrm{j}\zeta_{\mathrm{hr}}\Omega_{\mathrm{hr}} - \Omega_{\mathrm{hr}}^2}} \quad [6]. \qquad (2)$$

In Equation (2), $\Omega_{\mathrm{hr}} = f/f_{\mathrm{hr}}$, where f_{hr} is the Helmholtz resonance frequency. $\phi_{\mathrm{hr}} = V_{\mathrm{hr}}/V$ is the Helmholtz resonance filling ratio, which is defined to be the ratio between the resonator cavity volume V_{hr} and the unit cell volume $V = Sd_{\mathrm{hr}}$. The unit cell has a thickness

of d_{hr}. ζ_{hr} is the damping coefficient of the resonator. Lastly, $K_0 = \rho_0 c_0^2$ is the bulk modulus of air, where $\rho_0 = 1.2\,\mathrm{kg\,m^{-3}}$ and $c_0 = 343\,\mathrm{m\,s^{-1}}$ are the density and speed of sound in air, respectively. At frequencies near the Helmholtz resonance, the fluid surrounding the resonator has a very low effective bulk modulus and therefore acts almost like a vacuum, prohibiting sound wave propagation across the metamaterial and resulting in superior transmission loss.

The sound propagation through each effective medium layer is calculated with a transfer matrix, which is obtained by substituting Equations (1) and (2) into

$$\mathbf{T}_{\mathrm{cl}} = \begin{bmatrix} 1 & \mathrm{j}\omega\rho_{\mathrm{eff,cl}} d_{\mathrm{cl}} \\ 0 & 1 \end{bmatrix} \tag{3}$$

and

$$\mathbf{T}_{\mathrm{hr}} = \begin{bmatrix} \cos k_{\mathrm{eff,hr}} d_{\mathrm{hr}} & \mathrm{j} Z_{\mathrm{eff,hr}} \sin k_{\mathrm{eff,hr}} d_{\mathrm{hr}} \\ -\frac{\mathrm{j}\sin k_{\mathrm{eff,hr}} d_{\mathrm{hr}}}{Z_{\mathrm{eff,hr}}} & \cos k_{\mathrm{eff,hr}} d_{\mathrm{hr}} \end{bmatrix}, \tag{4}$$

where $Z_{\mathrm{eff,hr}}$ and $k_{\mathrm{eff,hr}}$ are the effective impedance and wavenumber of the Helmholtz resonator effective medium layer, respectively [7]. A global transfer matrix can be calculated through matrix multiplication of the transfer matrix from each effective medium and the transmission loss TL can be calculated from the elements of the global transfer matrix $\mathbf{T}_{\mathrm{TMM}}$, as described in Ref. [7].

The transmission loss of an example metamaterial design is calculated with the proposed effective medium method between 100 and 1000 Hz. The design used the following input parameters: $m_0'' = 5\,\mathrm{kg\,m^{-2}}$, $\phi_{\mathrm{cl}} = 0.15$, $S = 2500\,\mathrm{mm^2}$, $\zeta_{\mathrm{cl}} = 0.03$, $\rho\mathrm{cl} = 1240\,\mathrm{kg\,m^{-3}}$, $d_{\mathrm{cl}} = 3.4\,\mathrm{mm}$, $\phi_{\mathrm{hr}} = 0.2$, $d_{\mathrm{hr}} = 30\,\mathrm{mm}$, and $\zeta_{\mathrm{hr}} = 0.01$. The resulting transmission loss is plotted in Figure 2, which shows a TL peak at the structural resonance $f_{\mathrm{cl}} = 310\,\mathrm{Hz}$ and another one at the Helmholtz resonance $f_{\mathrm{hr}} = 388\,\mathrm{Hz}$. Each of these resonance mechanisms introduces a stop-band, leading to a TL improvement compared to the corresponding mass-law, as shown by the shaded blue region in the figure. However, certain frequencies between the structural resonance and Helmholtz resonance have TL deficits in comparison to the mass-law, as shown by the red colored regions in the figure. This is most notable at 340 Hz, which corresponds to a partition resonance due to the out-of-phase movement between the resonator and the host structure with minimum sound wave attenuation across the metamaterial.

Sensitivity Studies

To investigate how the TL performance of the metamaterial can be best improved, a sensitivity study is carried out to investigate the effect of key parameters on the TL of the metamaterial. To evaluate the performance of the metamaterial, the difference in transmission loss between the metamaterial and the corresponding mass-law is chosen as the figure of merit. This sensitivity study focuses on the following key parameters of the AMM: the cantilever mass ratio ϕ_{cl}, the Helmholtz resonance filling ratio ϕ_{hr} and the ratio between the two resonance frequencies $\phi_f = f_{\mathrm{hr}}/f_{\mathrm{cl}}$. These parameters influence Equations (1) and (2), which then influence the transmission loss performance of the metamaterial. All other input parameters to the effective medium model remained constant.

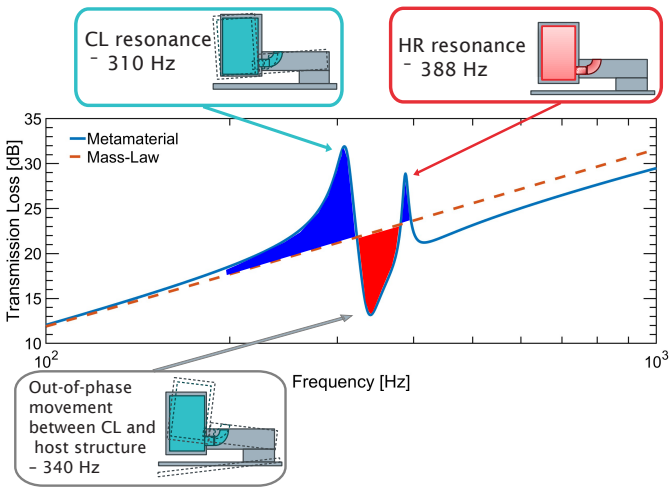

Figure 2: TL and equivalent mass-law TL of an example metamaterial design consisting of a cantilever resonator with an embedded Helmholtz resonator.

Cantilever Mass Ratio

Figure 3(a) shows a contour plot of the metamaterial TL improvement (compared to the mass-law), with varying values of the cantilever mass ratio on the x-axis. The cantilever mass ratio values range from 0 to 0.8 with a resolution of 0.01. The frequency, shown on the y-axis, is normalised to the structural resonance frequency. The blue and red colours correspond to TL improvements and TL deficits in comparison to the mass-law TL, respectively. Frequencies at which the TL of the AMM coincides with the mass-law are highlighted by the black contour line. Figure 3(b) shows the transmission loss of the metamaterial with a few selected mass ratio values. These results show that an increase in the mass ratio increases both the bandwidth and peak TL value of the structural resonance stop-band (at a normalised frequency of one). However, the figures also show that with higher mass ratio values, the TL dip effect becomes stronger and higher in frequency. This highlights a design trade-off between improving the structural resonance stop-band and reducing the strength of the TL dip.

The influence of mass ratio values on the TL performance of the Helmholtz resonator can be distinguished into four regions, as highlighted by each transmission loss curve in Figure 3(b): At low mass ratio values, the structural resonance and Helmholtz resonance stop-bands are separated (blue curve in Figure 3(b)). As the mass ratio increases, the TL dip frequency moves closer to the Helmholtz resonance frequency. The Helmholtz resonance (inducing a TL peak) partially reduces the strength of the partition resonance (inducing the TL dip). For certain mass ratio values, the Helmholtz resonance stop-band continues to reduce the TL dip, but drops below the mass-law (see red

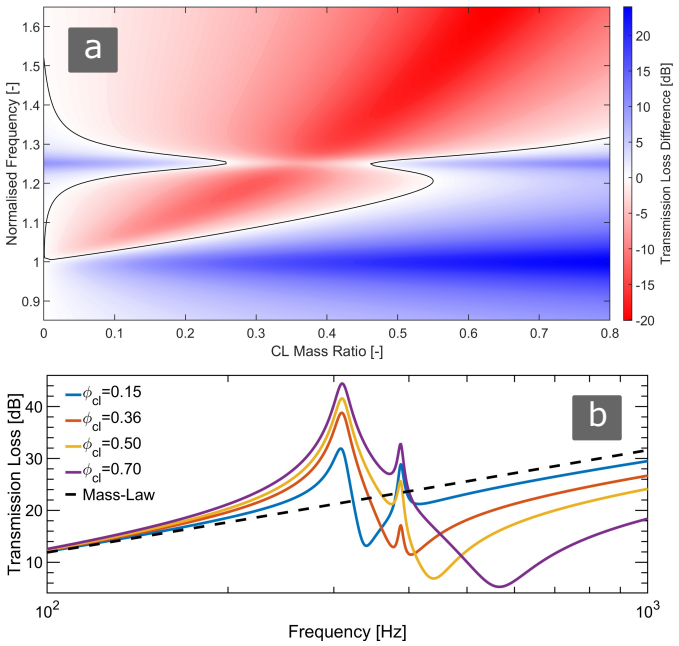

Figure 3: Sensitivity analysis results of the proposed metamaterial with varying cantilever mass ratio values. (a) Contour plot of the metamaterial TL improvement (compared to the the mass-law), with varying values of the cantilever mass ratio; (b) Transmission loss of the metamaterial partition with selected cantilever mass ratio values.

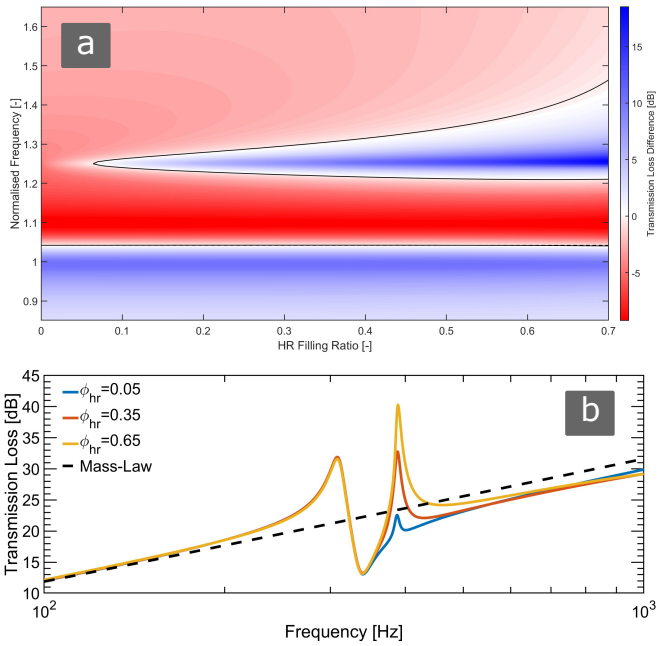

Figure 4: Sensitivity analysis results of the proposed metamaterial with varying Helmholtz resonance filling ratio values. (a) Contour plot of the metamaterial TL improvement (compared to the mass-law), with varying values of the Helmholtz resonance filling ratio; (b) Transmission loss of the metamaterial partition with selected Helmholtz resonance filling ratio values.

curve in Figure 3(b)). As the mass ratio increases further, the TL dip frequency increases above the Helmholtz resonance frequency, leading to the Helmholtz resonance stop-band re-emerging above the mass-law (see yellow curve in Figure 3(b)). For large enough mass ratio values, the Helmholtz resonance stop-band combines with the structural resonance stop-band to achieve a single stop-band with TL improvement above the mass-law (see purple curve in Figure 3(b)).

The sensitivity study results in Figure 3 indicate that a larger mass ratio is desirable for improving the TL within the structural resonance stop-band, especially when the Helmholtz resonance stop-band combines with the structural resonance bandwidth at higher mass ratio values. However, one factor to consider is that the increase of mass ratio values results in a more pronounced TL dip. Additionally, it could be difficult to practically implement AMM designs with very large mass ratio values.

Helmholtz Resonator Filling Ratio

Figure 4(a) shows a contour plot of the metamaterial TL improvement for varying values of the Helmholtz resonator filling ratio. The filling ratio values range from 0 to 0.7, with a resolution of 0.01. Figure 4(b) shows the transmission loss of the metamaterial with a few selected filling ratio values. Figure 4(a) shows that the increase in filling ratio values improve only the bandwidth and peak TL level of the Helmholtz resonance stop-band. At low filling ratios, the Helmholtz resonance stop-band has a very small bandwidth and low peak TL value and does not achieve TL values above the mass-law (see blue curve in Figure 4(b)). After a certain 'critical' filling ratio, the Helmholtz resonance peak emerges above the mass-law (see red curve in Figure 4(b)). With increasing filling ratio values, both the bandwidth and peak TL value of the Helmholtz resonator stop-band increases (see yellow curve in Figure 4(b)).

These results suggest that the filling ratio should be maximised for a broadband TL improvement. However, realising a metamaterial design with high filling ratios is not practical. This is because the resulting designs would require a very large Helmholtz resonance cavity, which would contradict the compact design philosophy that acoustic metamaterials offer.

Resonance Frequency Ratio

Figure 5(a) shows a contour plot of the metamaterial TL improvement for varying values of the resonance frequency ratio. The resonance frequency ratio $\phi_f = f_{\mathrm{hr}}/f_{\mathrm{cl}}$ varies between 0.5 to 1.5 with steps of 0.005. Figure 5(b) shows the transmission loss of the metamaterial with a few selected resonance frequency ratio values. The effect of the resonance frequency ratio on the transmission loss performance of the AMM can be categorized into five regions, as highlighted by each transmission loss curve in Figure 5(b): If the frequency ratio is below one, the Helmholtz resonance stop-band expands the structural resonance stop-band towards lower frequencies, but there is no TL improvement at the TL dip (see blue curve in Figure 5(b)). If the frequency ratio is slightly above one, the Helmholtz resonance stop-band extends the structural resonance stop-band towards higher frequencies and reduces the TL dip, as shown in the red

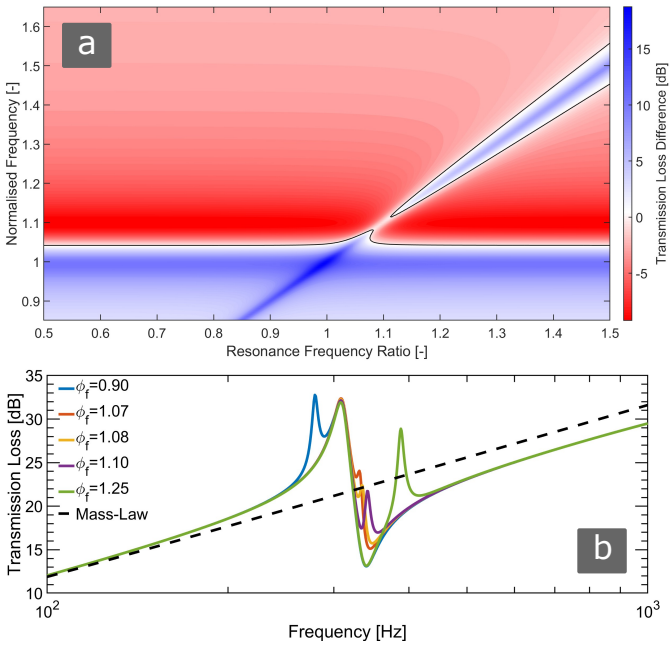

Figure 5: Sensitivity analysis results of the proposed metamaterial with varying resonance frequency ratio values. (a) Contour plot of the metamaterial TL improvement (compared to the mass-law), with varying values of the resonance frequency ratio; (b) Transmission loss of the metamaterial partition with selected resonance frequency ratio values.

curve of Figure 5(b). However, there is a trade-off between improving the structural resonance TL bandwidth and the reduction the TL dip strength. This is observed in the yellow curve in Figure 5(b), where the Helmholtz resonance stop-band is much weaker with only a fractional increase of the frequency ratio compared to the red curve. As the resonance frequency ratio continues to increase, the Helmholtz resonance stop-band further reduces the TL dip, achieving a maximum reduction when the Helmholtz resonance frequency coincides with the TL dip frequency. However, the Helmholtz resonance stop-band submerges below the mass-law, resulting in no TL improvement compared to the mass-law (see purple curve in Figure 5(b)). At higher resonance frequency ratio values, the Helmholtz resonance stop-band re-emerges above the mass-law, but become clearly separated from the structural resonance stop-band (see green curve in Figure 5(b)).

The sensitivity study results in Figure 5 show a trade-off between improving the TL bandwidth and reducing the TL dip. If the target of a design of the AMM is to achieve broadband TL improvement and reduce the TL deficit near the dip frequency, the two resonance frequencies should be tuned relatively closely together. However, practical constraints could limit realised designs with particular resonance frequency ratio values. This is especially the case for very low frequency ratio values, as the Helmholtz resonator is housed inside the cantilever and would require a larger Helmholtz resonator cavity to achieve a low resonance frequency.

Conclusions

To conclude, this paper presents sensitivity study results for a novel vibro-acoustic metamaterial design with an embedded Helmholtz resonator. This metamaterial aims to offer a compact design to improve the structural resonance bandwidth without introducing additional mass, achieved by a careful tuning of the Helmholtz resonance stop-band. Results from the sensitivity study indicate that the mass ratio and filling ratio should be maximised to offer a strong stop-band performance with greater bandwidth and TL improvement above the mass-law. However, large cantilever mass ratio values lead to very strong TL dips, which weaken the Helmholtz resonance performance when the Helmholtz resonance frequency is tuned closely to the TL dip frequency. Therefore, the resonance frequency ratio needs to be carefully considered for broadband TL improvement and the reduction of the TL dip. Nevertheless, these sensitivity studies help to provide a guideline on realising designs of the proposed metamaterial that show promise for improved broadband TL performance.

References

[1] L. Van Belle, C. Claeys, E. Deckers, and W. Desmet, The impact of damping on the sound transmission loss of locally resonant metamaterial plates, Journal of Sound and Vibration, vol. 461, p. 114909, Nov. 2019.

[2] D. Giannini, M. Schevenels, and E. P. B. Reynders, Rotational and multimodal local resonators for broadband sound insulation of orthotropic metamaterial plates, Journal of Sound and Vibration, vol. 547, p. 117453, Mar. 2023.

[3] N. G. R. de Melo Filho, L. Van Belle, C. Claeys, E. Deckers, and W. Desmet, Dynamic mass based sound transmission loss prediction of vibro-acoustic metamaterial double panels applied to the mass-air-mass resonance, Journal of Sound and Vibration, vol. 442, pp. 28–44, Mar. 2019.

[4] S. Janssen, L. Van Belle, N. G. R. de Melo Filho, W. Desmet, C. Claeys, and E. Deckers, Improving the noise insulation performance of vibro-acoustic metamaterial panels through multi-resonant design, Applied Acoustics, vol. 213, p. 109622, Oct. 2023.

[5] T. Yamamoto, Acoustic metamaterial plate embedded with Helmholtz resonators for extraordinary sound transmission loss, Journal of Applied Physics, vol. 123, no. 21, p. 215110, Jun. 2018,0.

[6] F. Langfeldt, H. Hoppen, and W. Gleine, Broadband low-frequency sound transmission loss improvement of double walls with helmholtz resonators, Journal of Sound and Vibration, vol. 476, p. 115309, Jun. 2020..

[7] J.-F. Allard and N. Atalla, Propagation of sound in porous media: modelling sound absorbing materials, 2nd ed. Hoboken, N.J: Wiley, 2009.